# ORIGINAL PAPER Open Access



# Polycarbonate nanocomposite thin films for EMI shielding: influence of CeNiO<sub>3</sub> and graphene nanoplatelets

Supreetha M.<sup>1,2</sup>, Veena M.G.<sup>2</sup>, Madhukar B.S.<sup>4</sup>, Pawandeep Kaur<sup>5</sup> and Gnana Prakash A.P.<sup>3\*</sup>

# **Abstract**

Polycarbonate (PC)-based nanocomposites reinforced with cerium nickelate (CeNiO<sub>3</sub>) and graphene nanoplatelets (GNP) were synthesized for enhanced electromagnetic interference (EMI) shielding applications. Morphological analysis through SEM and EDX confirmed uniform dispersion and elemental composition of the nanofillers. The structural and chemical interactions were validated using XRD and FTIR, indicating successful integration of CeNiO<sub>3</sub> and GNP into the polymer matrix. The AC conductivity, dielectric loss tangent, and magnetic loss tangent increased with higher filler loading, promoting effective energy dissipation. Among all compositions, the PC/4wt% CeNiO<sub>3</sub>@ 6wt% GNP nanocomposite exhibited the highest shielding effectiveness of 36.32 dB in the X-band (8.2–12.4 GHz), attributed to a synergistic balance between reflection and absorption mechanisms. The results of this study highlight the capabilities of CeNiO<sub>3</sub>-GNP hybrid fillers in producing high-performance materials for electromagnetic interference shielding in cutting-edge electronic applications.

Keywords Polycarbonate, Graphene nanoplatelets (GNP), EMI Shielding effectiveness, X-band, Hybrid nanofillers

# Introduction

The evolution of electronic communications technology has been remarkable, resulting in the extensive adoption of diverse electrical devices in numerous fields such as communications, public services, aviation, and military applications (Bheema et al. 2024; Sankaran et al. 2018). In addition, these electronic devices continuously emit

electromagnetic (EM) waves during operation, causing electromagnetic interference (EMI) with a range of electrical appliances, which negatively impacts the operational accuracy of electronic equipment in the electronics industry (Tong 2009). EMI shielding materials represent the most efficient method for protecting electronic devices and human health from the harmful effects of electromagnetic radiation.

Research on EMI shielding materials is increasingly advancing in the dynamic context of the fourth industrial revolution. A variety of EMI shielding materials, such as those made from metals, carbon, and the recently developed MXene (metal carbides, nitrides, or carbonitrides) materials, as well as their composites, have been recognized for their ability to improve EMI shielding effectiveness (Nguyen and Choi 2024). Polymer nanocomposites (PNCs) can be specifically designed to suppress electromagnetic radiation, influenced by the type of polymer and filler employed. Their desirable characteristics have led to the consideration

gnanaprakash@physics.uni-mysore.ac.in

<sup>&</sup>lt;sup>5</sup> Department of Electronics Technology, Guru Nanak Dev University, Amritsar 143005, India



© The Author(s) 2025. **Open Access** This article is licensed under a Creative Commons Attribution 4.0 International License, which permits use, sharing, adaptation, distribution and reproduction in any medium or format, as long as you give appropriate credit to the original author(s) and the source, provide a link to the Creative Commons licence, and indicate if changes were made. The images or other third party material in this article are included in the article's Creative Commons licence, unless indicated otherwise in a credit line to the material. If material is not included in the article's Creative Commons licence and your intended use is not permitted by statutory regulation or exceeds the permitted use, you will need to obtain permission directly from the copyright holder. To view a copy of this licence, visit http://creativecommons.org/licenses/by/4.0/.

<sup>\*</sup>Correspondence: Gnana Prakash A.P.

<sup>&</sup>lt;sup>1</sup> Department of Studies in Electronics, PG Center, Hemagangotri, University of Mysore, Hassan 573220, India

<sup>&</sup>lt;sup>2</sup> Department of Electronics and Communication Engineering, JSS Science and Technology University, Sri Jayachamarajendra College of Engineering, Mysuru 570006, India

 $<sup>^3</sup>$  Department of Studies in Physics, Manasagangotri, University of Mysore, Mysuru 570006, India

Department of Chemistry, JSS Science and Technology University, Sri Jayachamarajendra College of Engineering, Mysuru 570006, India

M. et al. J Mater. Sci: Mater Enq. (2025) 20:142 Page 2 of 13

of PNCs as a potential replacement for metals in the field of EMI shielding (Bhaskaran et al. 2020; Uma Varun et al. 2019; Rajesh Kumar and Etika 2022; Bheema et al. 2022). Polymer nanocomposites that incorporate lossy dielectric or magnetic materials are utilized to mitigate electromagnetic interference and protect electronic devices from undesirable electromagnetic waves by means of reflection and absorption. Generally, shielding materials that focus on absorption are preferred for equipment since reflection can introduce additional interference to nearby devices (Choudhary et al. 2020).

The process of material selection plays a significant role in the formulation of EMI shielding materials. Recent investigations highlight a surge in the demand for budgetfriendly and effective EMI shielding solutions, mainly due to the expanding integration of electronic devices and electrical systems in various industrial applications (Zhang et al. 2019; Vyas and Chandra 2019; Ramakrishna et al. 2024; Pasha et al. 2023). The addition of 0.5 wt% graphene nanoplatelets (GNP) to polycarbonate (PC) and its foaming with supercritical CO<sub>2</sub> resulted in a specific EMI shielding effectiveness (SE) of about 39 dB·cm<sup>3</sup>/g, which is 35 times superior to that of the unfoamed samples (Gedler et al. 2016). Authors fabricated polycarbonate/GNP nanocomposites via solution mixing and hot compaction, featuring up to 6 wt% GNP. The sample with a 2 mm thickness and GNP volume fraction of 0.037 demonstrated an EMI SE of 47.2 dB. The effective dispersion of GNP in the polycarbonate is responsible for the low percolation threshold (Nimbalkar et al. 2018).

The flexural properties and electromagnetic interference shielding effectiveness (EMI SE) of polycarbonate (PC) composites that are reinforced with multi-walled carbon nanotubes (MWCNT) and heat-treated expanded graphite (eG) are examined. They showed that the EMI SE increased as the filler content increases with an average EMI SE surpassing 20 dB for mixtures with over 10 wt% filler (Lee et al. 2021). PVC/PMMA/GNPs/MMT/CuO nanocomposites are prepared using the solvent-casting technique. The SE<sub>Total</sub> is achieved up to  $\sim\!5$  dB in the 8–12 GHz range for the 2.5 wt% GNPs-loaded nanocomposite (Rani and Khadheer Pasha 2024). The reduced bandgap variant of CeNiO $_3$  from 1.48 eV to 1.77 eV for photovoltaic applications gives an increased conductivity contributing to improve EMI SE (Barad et al. 2018).

With the several research article surveys, literature on hybrid nanofillers are found to be scanty. Hence, in the present study, hybrid nanofillers with varying concentrations of GNP and perovskite  ${\rm CeNiO_3}$  are investigated in polymer thin films. This study describes the electrical, EMI shielding, and morphological characteristics of the fabricated nanocomposite film.

# **Methods and materials**

The commercial grade Polycarbonate (PC) granules with a purity of 99% were used as the base polymer. The chemicals Cerium nitrate hexahydrate (Ce(NO<sub>3</sub>)<sub>3</sub> 0.6H<sub>2</sub>O), nickel nitrate hexahydrate (Ni(NO<sub>3</sub>)<sub>2</sub>. 6H<sub>2</sub>O) were purchased in high purity from s d-fine Chem Limited. The GNP with the particle size of 25 µm were purchased from Sigma Aldrich. The nanoparticles of cerium nickelate (CeNiO<sub>3</sub>) were synthesized using the solution combustion method. For the synthesis, 4.3 g of cerium nitrate, 2.90 g of nickel nitrate, and 2.67 g of glycine as a precursor are taken in a beaker with 50 ml of water. The beaker is placed on the magnetic stirrer at a temperature of 90 °C. Then the magnetic stirrer is rotated at the speed of 450-500 rpm for 3 to 4 h until the semi-liquid jelly material is formed. Finally, the materials obtained are calcinated in the red-hot crucible at 500 °C for 1 h to obtain the nanoparticles. The nanoparticles obtained were weighed using an electronic balance resulting in 1.22 g.

The solution casting method is used to prepare PC/ CeNiO<sub>3</sub>@GNP nanocomposites of different compositions, namely 0.0, 2.8, 4.6, 6.4, and 8.2 (wt/wt%). Polycarbonate solution is prepared by weighing 2 g of PC granules and dissolving them in 100 ml of dichloromethane solvent, stirred well with a speed of 500 rpm using a magnetic stirrer for 45 min at room temperature. Subsequently, the determined quantity of CeNiO<sub>3</sub>@GNP was measured and incorporated into the polycarbonate solution. In order to ensure uniform distribution, the solution is vigorously agitated at room temperature with a magnetic stirrer and then followed by ultra-sonication for 30 min, so that the uniform dispersion of nanoparticles takes place in the polymer solution. Eventually, the nanocomposite solution is poured into a pristine glass mold, allowing the solvent to evaporate completely. After the solvent had fully evaporated, the films were cautiously detached from the mould. The nanocomposite films produced were used for characterization.

# **Results and discussions**

The morphological, electrical, and shielding effectiveness investigations were undertaken for the samples. The discussions are elaborated in the subsequent sections.

## **SEM with EDX**

The Scanning Electron Microscopy (SEM) with Energy Dispersive X-Ray Analysis (EDX) was carried out to investigate the particle size and morphology of thin films and nanoparticles used as fillers. Figure 1a shows the surface morphology of pristine polycarbonate (PC). The surface appears smooth and featureless, which is characteristic of amorphous thermoplastics. The absence of any particulate or crystalline domains confirms the

M. et al. J Mater. Sci: Mater Eng. (2025) 20:142 Page 3 of 13

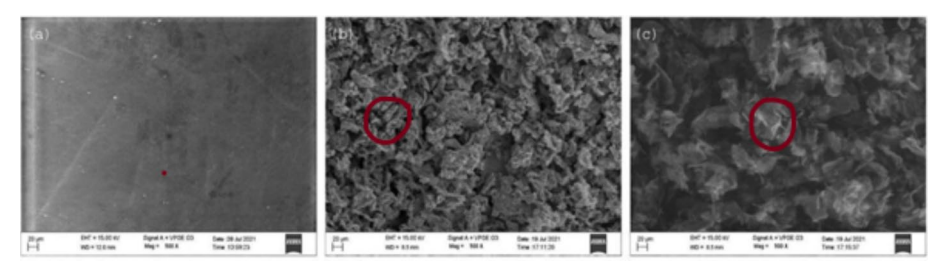


Fig. 1 SEM images of a base polymer PC, b synthesized CeNiO<sub>3</sub> nanoparticles, and c GNP

homogeneous nature of the neat matrix. The microstructure of synthesized  $CeNiO_3$  nanoparticles, with an average particle size of 236 nm, is represented in Fig. 1b. The SEM reveals a clustered granular morphology, with particles appearing as dense, irregularly shaped aggregates. These agglomerates are indicative of nanoparticles with high surface energy, which may tend to clump together post-synthesis. The grain-like texture and nanoscale features are favorable for enhancing interfacial polarization, which is essential for dielectric and magnetic loss contributions in EMI shielding applications.

Figure 1c illustrates the morphology of GNP, exhibiting thin, wrinkled, and sheet-like structures with an average thickness of  $6{\text -}8~\mu m$ . The layered or flake-like appearance with overlapping platelets confirms the successful exfoliation of GNP. This 2D morphology provides a high aspect ratio and large surface area, promoting the formation of effective conductive networks and facilitating electron transport, both of which are critical for reflection-based EMI shielding.

Figure 2 presents SEM micrographs of PC/CeNiO<sub>3</sub>@ GNP nanocomposites at varying filler loadings and magnifications. The images provide insight into the dispersion quality, surface morphology, and microstructural uniformity of the hybrid fillers within the polycarbonate matrix.

Figure 2a reveals moderate agglomeration of CeNiO<sub>3</sub> nanoparticles distributed throughout the PC matrix. These dark regions are attributed to CeNiO<sub>3</sub> clusters embedded in the polymer. Figure 2b depicts a sample with higher CeNiO<sub>3</sub> loading or reduced GNP content. A denser distribution of larger aggregates is observed, indicating more pronounced clustering. The occurrence of such agglomeration can cause irregularities in electrical pathways, yet it promotes dielectric loss through interfacial polarization, which benefits absorption-dominant EMI shielding. Figure 2c highlights a well-dispersed, flake-like morphology. This configuration allows for the development of seamless conductive networks, which are important for advancing both electrical conductivity and

shielding effectiveness through reflection and absorption techniques.

Overall, the SEM analysis confirms that the sample corresponding to Fig. 2c—with well-dispersed GNP and moderate CeNiO<sub>3</sub> content—exhibits the most favorable morphology for EMI shielding applications. The synergistic effect of 2D conductive graphene and dielectric CeNiO<sub>3</sub> nanoparticles is evident in the uniform distribution and interfacial compatibility observed across the micrographs.

Figure 3a represents the EDX profile of C and O of the polycarbonate thin film, which is the base polymer. Figure 3b and c represent the EDX profile of Ce, Ni, and O of the synthesized CeNiO $_3$  and C of GNP, respectively. The results of the EDX analysis are shown with the spectrum. Figure 4 represents the EDX analysis of PC/CeNiO $_3$ @ GNP thin films with different filler concentrations. The profile indicates the presence of C, Ce, Ni, and O in all the fabricated samples.

# XRD analysis

The XRD patterns of pure PC and CeNiO<sub>3</sub>/GNP nanocomposites are depicted in. The 2θ value at 16° shows the amorphous nature of the polycarbonate (PC). As the addition of the nanoparticle to the polymer in different concentrations occurs, there is a slight shift in the peak which may be attributed to the interaction of the incorporated nano filler (CeNiO<sub>3</sub>/GNP) with the polymer (PC) matrix. By adding the nanoparticle to the polymer, the additional peak observed at  $2\theta = 26^{\circ}$  is due to the presence of CeNiO<sub>3</sub>. The peak at  $2\theta = 28^{\circ}$  and  $56^{\circ}$  confirms the presence of the GNP (Rashad et al. 2014). The diffraction peak at  $2\theta$ : 26.7°, 33.2°, 56.2°, and 72.3° is related to the perovskite CeNiO<sub>3</sub> nanoparticles (Dehghani et al. 2020). As we observed from Fig. 5, as the concentration of the CeNiO<sub>3</sub> increases, the intensity of the polymer peak decreases. XRD intensity and peak clarity reveal how well CeNiO<sub>3</sub>@GNP is integrated in the PC matrix. The sample with the sharpest crystalline features (PC/4wt% CeNiO<sub>3</sub>@6wt% GNP) shows maximum shielding, driven by an optimized microstructure that enhances M. et al. J Mater. Sci: Mater Enq. (2025) 20:142 Page 4 of 13

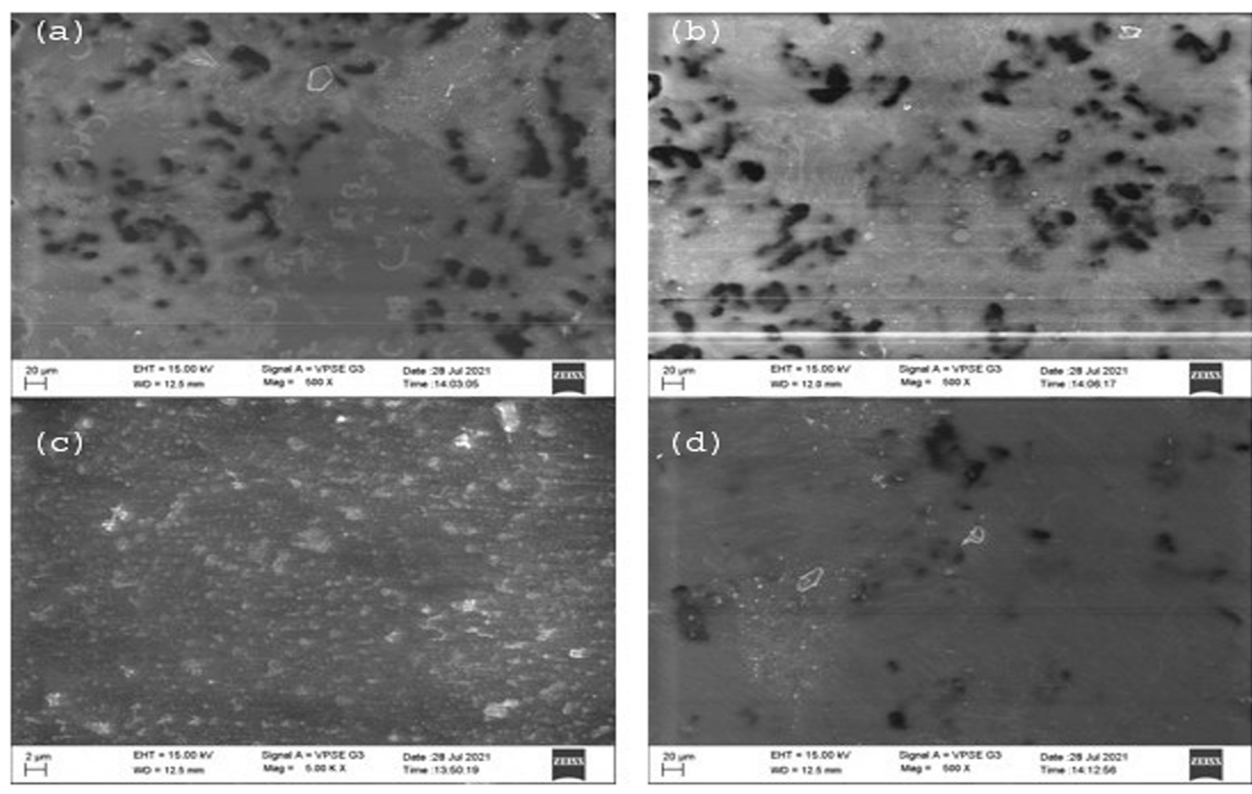


Fig. 2 SEM Images of PC/CeNiO<sub>3</sub>@GNP nanocomposites

dielectric and conductive losses, matching the SEA-dominant behavior indicating optimal dispersion and phase interaction at this composition. As the XRD intensity decreases (e.g., in PC/8wt%CeNiO $_3$ @2wt%GNP), both SE $_{\rm A}$  and SE $_{\rm T}$  also decrease, suggesting a decline in effective shielding.

XRD intensity and peak clarity reveal how well CeNiO $_3$ @ GNP is integrated in the PC matrix. The sample with the sharpest crystalline features (PC/4wt%CeNiO $_3$ @6wt%GNP) shows maximum shielding, driven by optimized microstructure that enhances dielectric and conductive losses, matching the SEA-dominant behavior in EMI data. The PC/4wt%CeNiO $_3$ @6wt%GNP sample shows the highest XRD intensity and also the maximum SET and SEA, indicating optimal dispersion and phase interaction at this composition. As the XRD intensity decreases (e.g., in PC/8wt%CeNiO $_3$ @2wt%GNP), both SEA and SET also decrease, suggesting a decline in effective shielding likely due to poor dispersion or agglomeration.

# FTIR analysis

The interaction between the nano filler added and the functional group present in the polymer can be evaluated by using Fourier Transform Infrared Spectroscopy (FT-IR). It is observed from the spectra in Fig. 6 that the

peak at 1155 cm<sup>-1</sup> is due to the C-O bond stretching, and another observed peak at 1383 cm<sup>-1</sup> is due to the C-H bending vibration. The C=C stretching appears at 1660 cm<sup>-1</sup> and 1492 cm<sup>-1</sup> due to the aromatic ring carbon; the peak at 1761 cm<sup>-1</sup> is due to C=O. Additionally, peaks at 2859 cm<sup>-1</sup> and 2947 cm<sup>-1</sup> correspond to C-H stretching of sp<sup>3</sup> and sp<sup>2</sup> hybridized carbon atoms, respectively. The C-C bond stretching is due to other peaks present at the fingerprint region (400–1400 cm<sup>-1</sup>). GNP interaction is evident from changes in the C=O and C-O-C vibrations. The existence of CeNiO<sub>3</sub> and GNP in the polymer (PC) led to a decrease in the intensity of the peak at 1757 cm<sup>-1</sup>, 1473 cm<sup>-1</sup>, 1145 cm<sup>-1</sup>, 987 cm<sup>-1</sup>, and 813 cm<sup>-1</sup>. The higher GNP content could result in more interactions with PC, possibly reducing intensity due to conductivity and absorption effects.

FTIR confirms the sample with optimal filler ratio promotes both conductive ( $SE_R$ ) and polarization-based ( $SE_A$ ) shielding mechanisms. The PC/4wt%CeNiO<sub>3</sub>@6wt%GNP shows the highest FTIR band intensity and the maximum  $SE_A$  and  $SE_T$ . This supports that strong Ce–O and Ni–O bonding, indicative of good dispersion and interaction with the matrix, enhances EMI shielding, especially by absorption. As FTIR intensity decreases, both SEA and SET decline,

M. et al. J Mater. Sci: Mater Eng. (2025) 20:142 Page 5 of 13

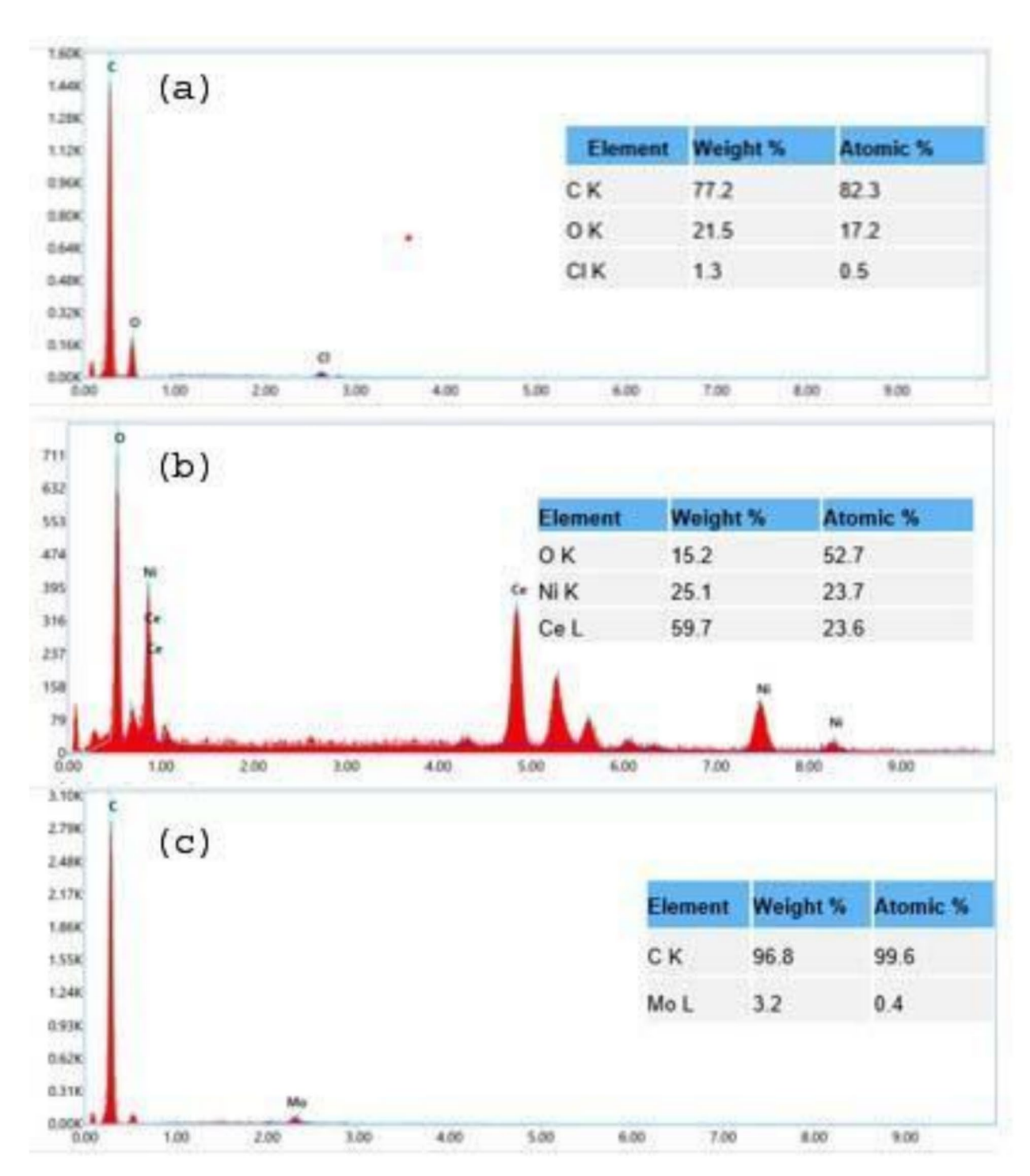


Fig. 3 EDX Analysis of a base polymer PC, b synthesized CeNiO<sub>3</sub> nanoparticles, and c GNP

confirming that interfacial polarization (linked to FTIR-active vibrations) is critical for effective EMI absorption (Fig. 6).

# AC conductivity $(\sigma_{ac})$

AC conductance of the samples were measured using Hioki HiTESTER 3532 LCR meter in a frequency range from 50 Hz to 5 MHz. The sample size of 20 mm diameter with a thickness of 0.05 mm was placed between

M. et al. J Mater. Sci: Mater Eng. (2025) 20:142 Page 6 of 13

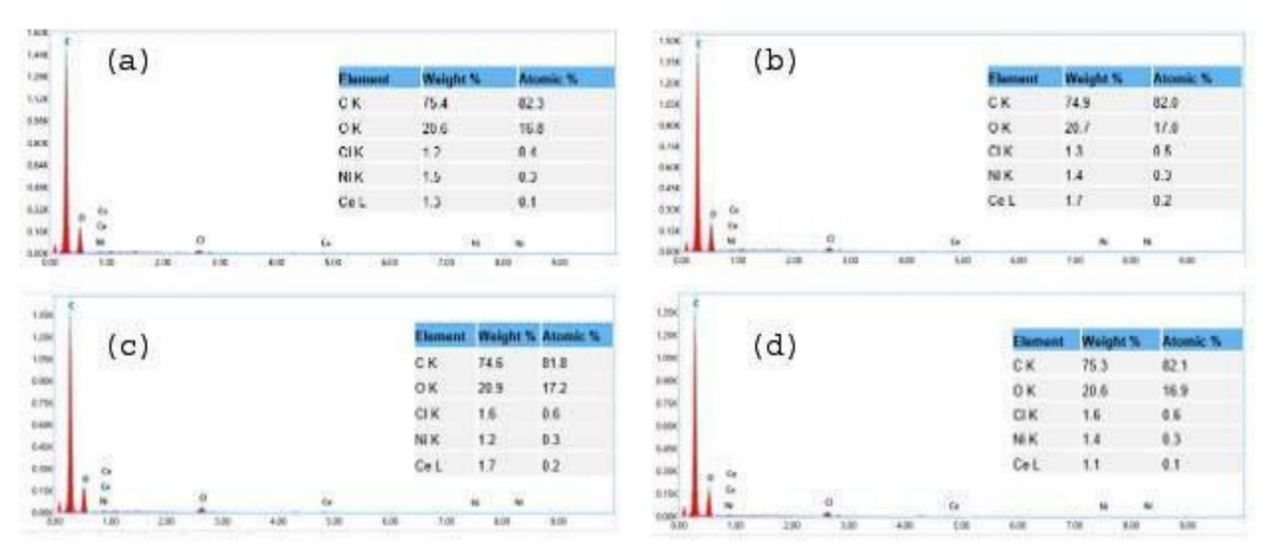


**Fig. 4** EDX Analysis of PC/CeNiO<sub>3</sub>@GNP nanocomposites

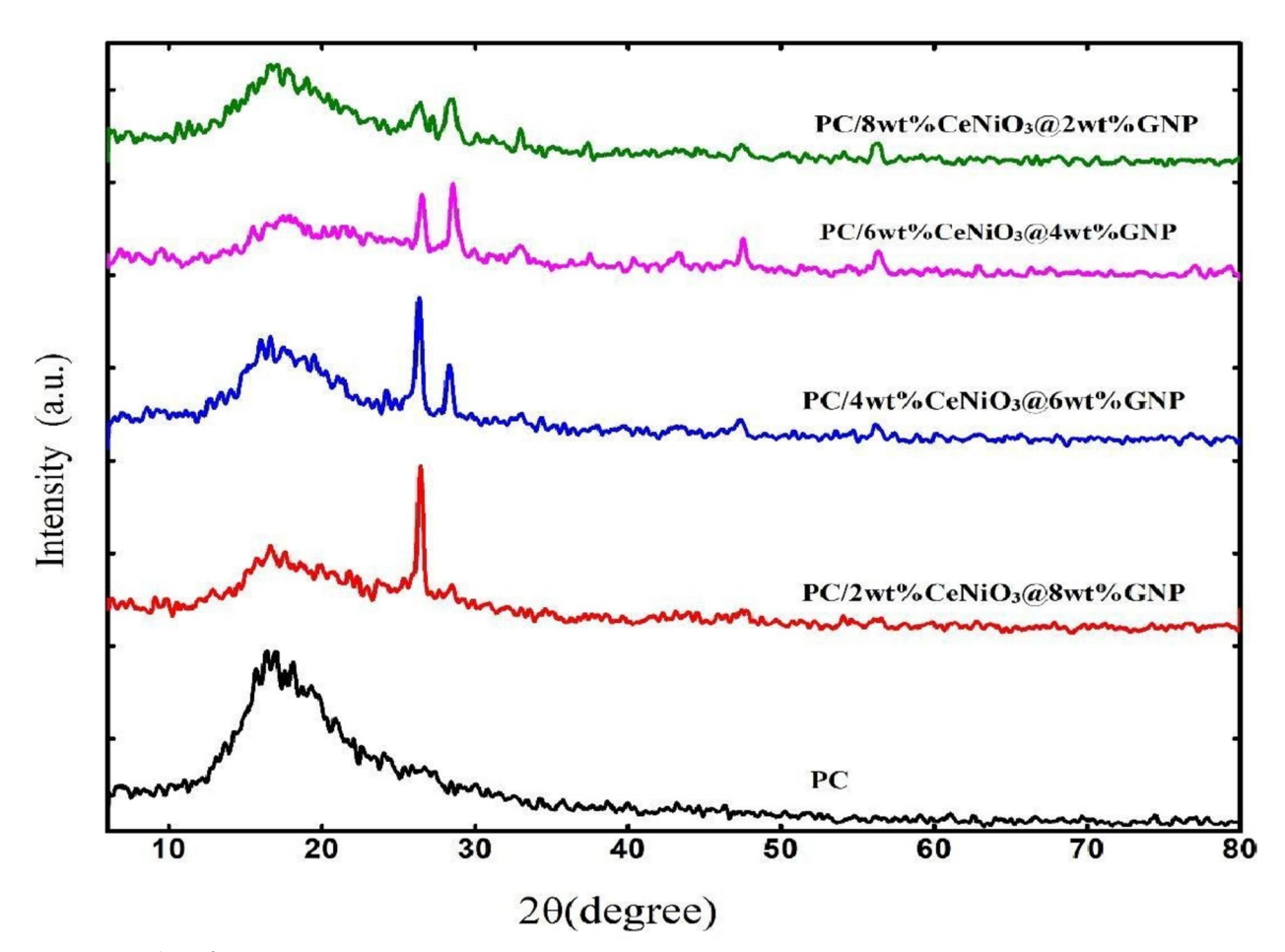


Fig. 5 XRD Analysis of PC/CeNiO<sub>3</sub>@GNP nanocomposites

M. et al. J Mater. Sci: Mater Eng. (2025) 20:142 Page 7 of 13

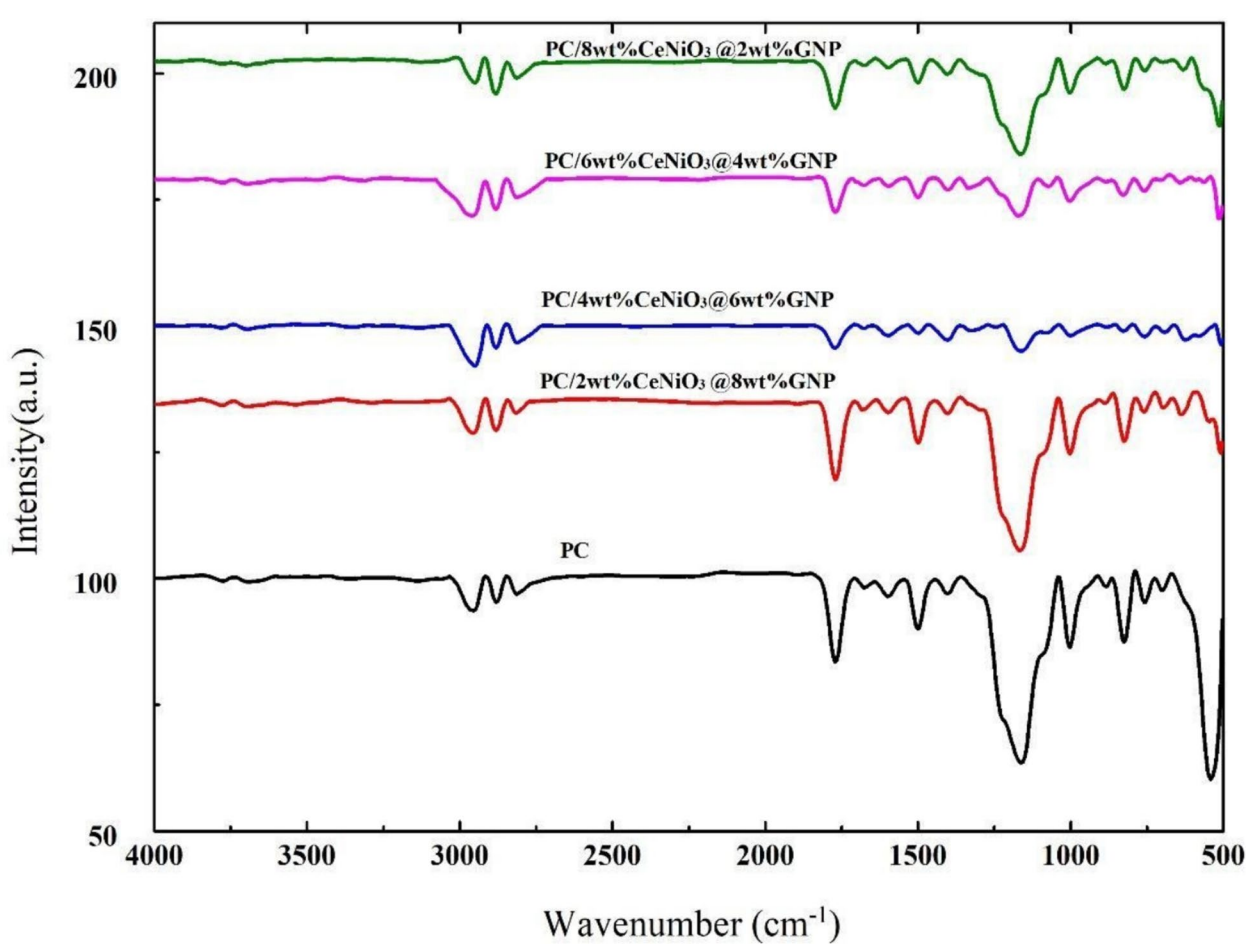


Fig. 6 FTIR Analysis of PC/CeNiO<sub>3</sub>@GNP nanocomposites

electrodes for measurement. Figure 7 shows the AC conductivity of the polymer thin films with varying filler loading as a function of frequency. It is observed that with higher GNP loading, AC conductivity increases. High AC conductivity generally enhances EMI shielding effectiveness (SE) because materials with better conductivity form more efficient charge transport networks, leading to stronger reflection (SE<sub>R</sub>) and absorption (SE<sub>A</sub>). Absorption-dominated shielding benefits more from interfacial polarization, magnetic/dielectric losses, and moderate  $\sigma_{sc}$ , as seen in PC/4wt%CeNiO<sub>3</sub>@6wt%GNP. The optimal shielding arises when there is a balance between conductive pathways and dielectric interfaces between the nanofillers and polymer chain.

# **Shielding effectiveness**

The shielding effectiveness for the prepared thin films has been calculated using the following equation.

$$SE_T = SE_A + SE_R + SE_M (1)$$

where  $SE_T$  is the total shielding effectiveness

SE<sub>A</sub> is shielding effectiveness due to absorption:

$$SE_A = -10 \log(1 - A_{eff}) \tag{2}$$

SE<sub>R</sub> is shielding effectiveness due to reflection:

$$SE_R = -10 \log(1 - R) \tag{3}$$

where  $A_{eff}$  is the effective absorption of the EM wave absorber, and is calculated using Eq. (4)

$$Aeff = \frac{1 - R - T}{1 - R} \tag{4}$$

Reflection coefficient (R) =  $|S_{11}|^2 = |S_{22}|^2$ 

where  $S_{11}$  represents the input reflection coefficient when the network's output is terminated by a matched load, and  $S_{22}$  is the output reflection coefficient.

Transmission coefficient

$$(T) = |S_{12}|^2 = |S_{21}|^2 \tag{5}$$

M. et al. J Mater. Sci: Mater Enq. (2025) 20:142 Page 8 of 13

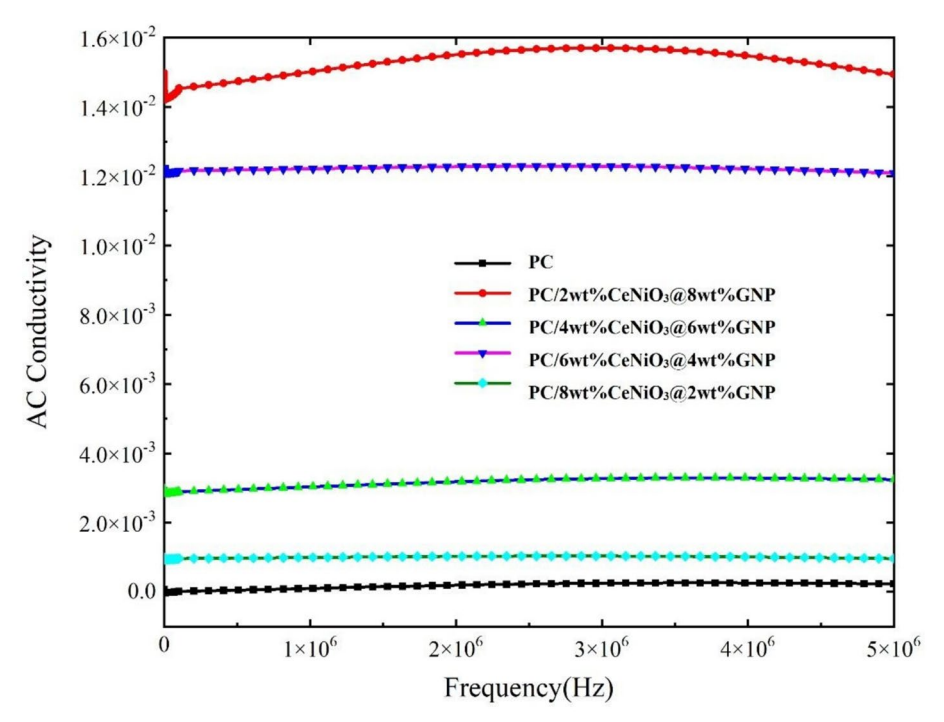


Fig. 7 AC Conductivity of PC/CeNiO<sub>3</sub>@GNP nanocomposites

 $SE_M$  is the shielding effectiveness due to multiple internal reflection, and  $SE_M$  can be neglected when the total shielding efficiency is greater than -10 dB. Then Eq. (1) becomes  $SE_T = SE_A + SE_R$ .

The shielding effectiveness was measured in the X-band (8.2–12.4 GHz) frequency range using the Agilent N522A vector network analyzer. The polymer nanocomposite with filler concentrations of 6 wt%, 4 wt% and 4 wt%, 6 wt% of CeNiO $_3$  and GNP exhibits a higher SE $_R$ , as shown in Fig. 8a. Shielding effectiveness due to reflection results from the conductive networks, meaning GNP contributes significantly to SE $_R$ . The polymer nanocomposite with filler concentrations of 4 wt%, 6 wt% and 6 wt%, 4 wt% of CeNiO $_3$  and GNP exhibits a higher SE $_A$ , as indicated in Fig. 8b. This indicates that increasing CeNiO $_3$  enhances absorption due to its dielectric and conductive nature.

Figure 8a and c show the observed maximum SER and SET of 12.41 dB at 8.36 GHz and 36.32 dB at 8.39 GHz for the polymer thin film with filler concentrations of 4 wt% and 6 wt% of  $\text{CeNiO}_3$  and GNP, respectively. The measured value of SEA is as shown in Fig. 8b; the maximum value is found to be 27.9 dB at 8.36 GHz for the sample with filler concentrations of 4 wt% and 6 wt% of  $\text{CeNiO}_3$  and GNP, respectively.

Table 1 summarizes the EMI shielding effectiveness of the PC-based polymer nanocomposites. The PC/4wt%CeNiO<sub>3</sub>@6wt%GNP sample demonstrates the highest EMI SE (36.32 dB) among all studies listed,

highlighting the synergistic effect of GNP for conductivity and  $\text{CeNiO}_3$  for dielectric/magnetic losses. The polymer nanocomposite with a filler concentration of 4wt%, 6wt% of  $\text{CeNiO}_3$  and GNP shows the highest shielding effectiveness across the frequency range, suggesting an optimal balance between absorption and reflection. The pure PC has the lowest SE, as expected, since it lacks conductive fillers. Higher GNP content increases  $\text{SE}_R$ , while higher  $\text{CeNiO}_3$  enhances  $\text{SE}_A$ . The trend suggests that a balanced ratio of  $\text{CeNiO}_3$  and GNP improves shielding. A higher value of EMI shielding effectiveness indicates better EMI shielding performance.

# Dielectric loss tangent

The real part of the permittivity ( $\epsilon'$ ) indicates the material's ability to store electrical energy. The highest  $\epsilon'$  values are observed for PC/CeNiO<sub>3</sub>@GNP with 2 wt% and 8 wt%, as shown in Fig. 9a, suggesting strong polarization effects. The imaginary part of the permittivity ( $\epsilon'$ ) represents energy dissipation due to dielectric losses. The highest  $\epsilon''$  values are observed for polymer nanocomposites with 2 wt%, 8 wt% and 4 wt%, 6 wt% nanocomposites, as shown in Fig. 9b. Peaks in  $\epsilon'$  correlate with relaxation processes, particularly around 9 GHz and 10 GHz. The nanocomposite with 2 wt% and 8 wt% shows the highest overall tan  $\delta$ , consistent with its high  $\epsilon''$  and  $\epsilon'$ .

M. et al. J Mater. Sci: Mater Eng. (2025) 20:142 Page 9 of 13

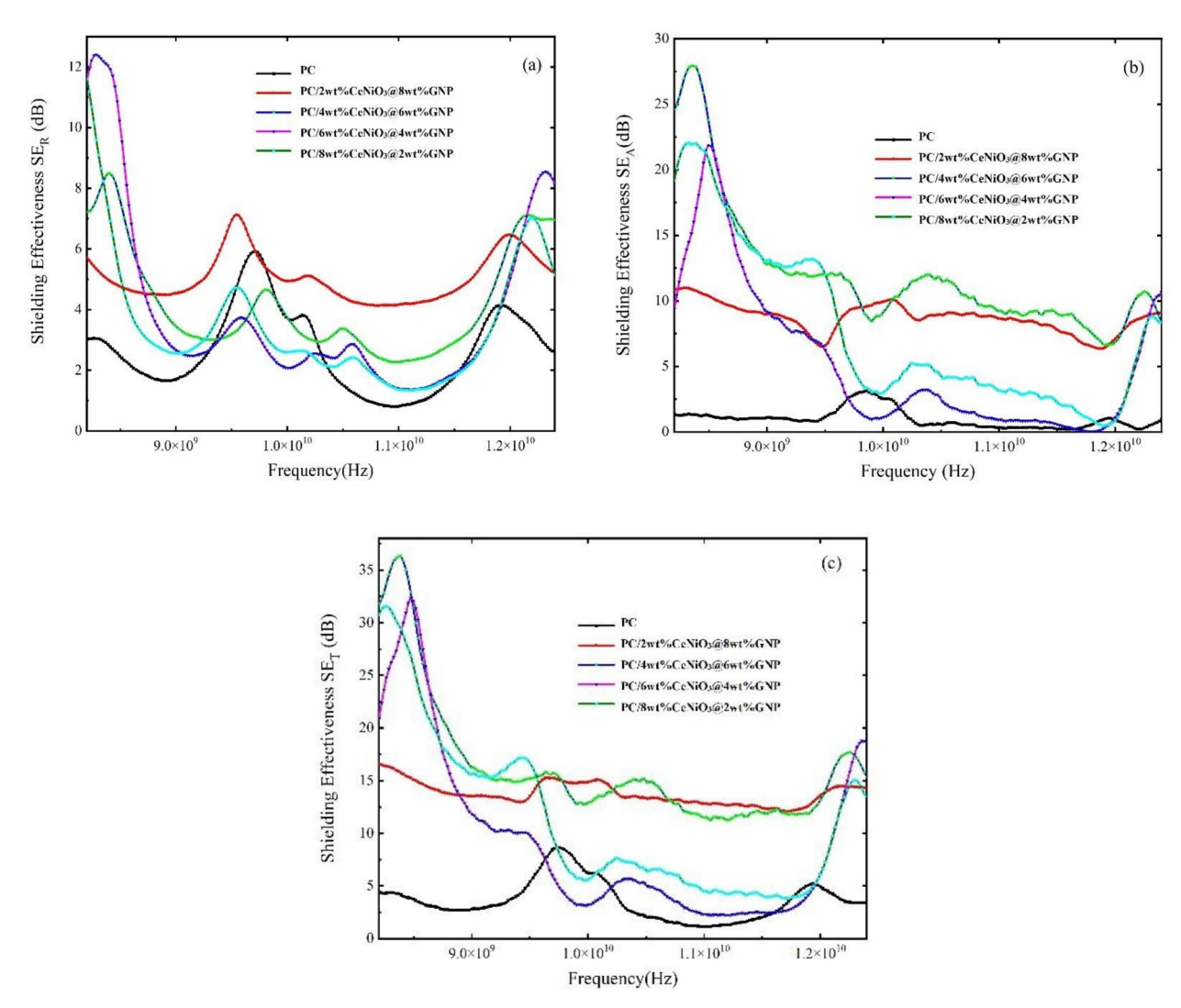


Fig. 8 a EMI shielding effectiveness due to reflection, **b** EMI shielding effectiveness due to absorption, **c** EMI shielding effectiveness due to total shielding effectiveness of PC/CeNiO<sub>3</sub>@GNP

The dielectric loss tangent (tan  $\delta_E$ ) is directly related to the real ( $\epsilon'$ ) and imaginary ( $\epsilon''$ ) parts of permittivity through the equation:

$$tan\delta E = \frac{\varepsilon \prime \prime}{\varepsilon \prime} \tag{6}$$

The dielectric loss tangent (tan  $\delta$ ) graph shows the energy dissipation characteristics of different PC (Polycarbonate) composite samples as a function of frequency. Polymer nanocomposite with 2 wt%, 8 wt% filler shows consistently high dielectric loss compared to other nanocomposites, as indicated in. This shows that with a higher concentration of GNP, there is a corresponding increase in dielectric loss, owing to the conductive nature of GNP. The polymer nanocomposites with filler concentrations of 6 wt%, 4 wt% and 8 wt%,

2 wt% of CeNiO<sub>3</sub>, GNP show moderate dielectric loss, but with different peak intensities, indicating a shift in dielectric behavior with changing filler content. Peaks in the dielectric loss tangent suggest strong dipolar relaxation and Maxwell-Wagner interfacial polarization (Wang Tong et al. 2017).

The highest loss values for most compositions appear around 9–10 GHz, indicating that this frequency range is critical for energy dissipation. The loss tangent behavior suggests that a balanced composition of CeNiO<sub>3</sub> and GNP is crucial to optimize dielectric properties. The observed peaks and shifts in dielectric loss suggest strong polarization mechanisms, which contribute to absorption-based EMI shielding.

M. et al. J Mater. Sci: Mater Eng. (2025) 20:142 Page 10 of 13

 Table 1
 Summary of PC-based nanocomposites for EMI shielding applications

SI. No	Filler	Processing	SE <sub>T</sub> in dB	Reference
1.	CNT (5 wt%)	Compression molding melt mixing	~-24	Arjmand et al. 2011)
2.	CNT (10 wt%)	Compression molding, solvent casting	-35	Pande et al. 2014)
3.	CNT (10 wt%)		-21	Pande et al. 2014)
4.	CNT (2 wt%)	Compression molding, solution blending	-23.1	Maiti et al. 2014)
5.	GNP/CNT (3:2 by wt) (4 wt%)	Melt mixing at high T (330 °C), compression molding	-21.6	Maiti and Khatua 2016)
6.	4 wt% CNT/5 wt% rGO-Fe <sub>3</sub> O <sub>4</sub> ran- dom dispersion	Solution approach, followed by hot press	-35.5	Yu et al. 2020)
7.	4 wt% CNT compartment approach		-33.2	Yu et al. 2020)
8.	4 wt% CNT random dispersion		-31	Yu et al. 2020)
9.	10 phr -CNT	Melt blending	~-26	Bagotia et al. 2017)
10.	15 phr- IrGO	Melt blending	~-30	Bagotia et al. 2018)
11.	10 phr- graphene/CNT hybrid (1:3)	Melt blending	~-34	Bagotia et al. 2019)
12.	10 phr- graphene		~-23	Bagotia et al. 2019)
13.	10 phr- CNTs		~-25	Bagotia et al. 2019)
14.	ITO/Au/ITO	Multilayer sputter-deposited film	-26.8	Erdogan et al. 2020)
15.	4wt%CeNiO <sub>3</sub> /6wt%GNP	Solution casting	36.32	This work
16.	6wt%CeNiO <sub>3</sub> /4wt%GNP		33	This work

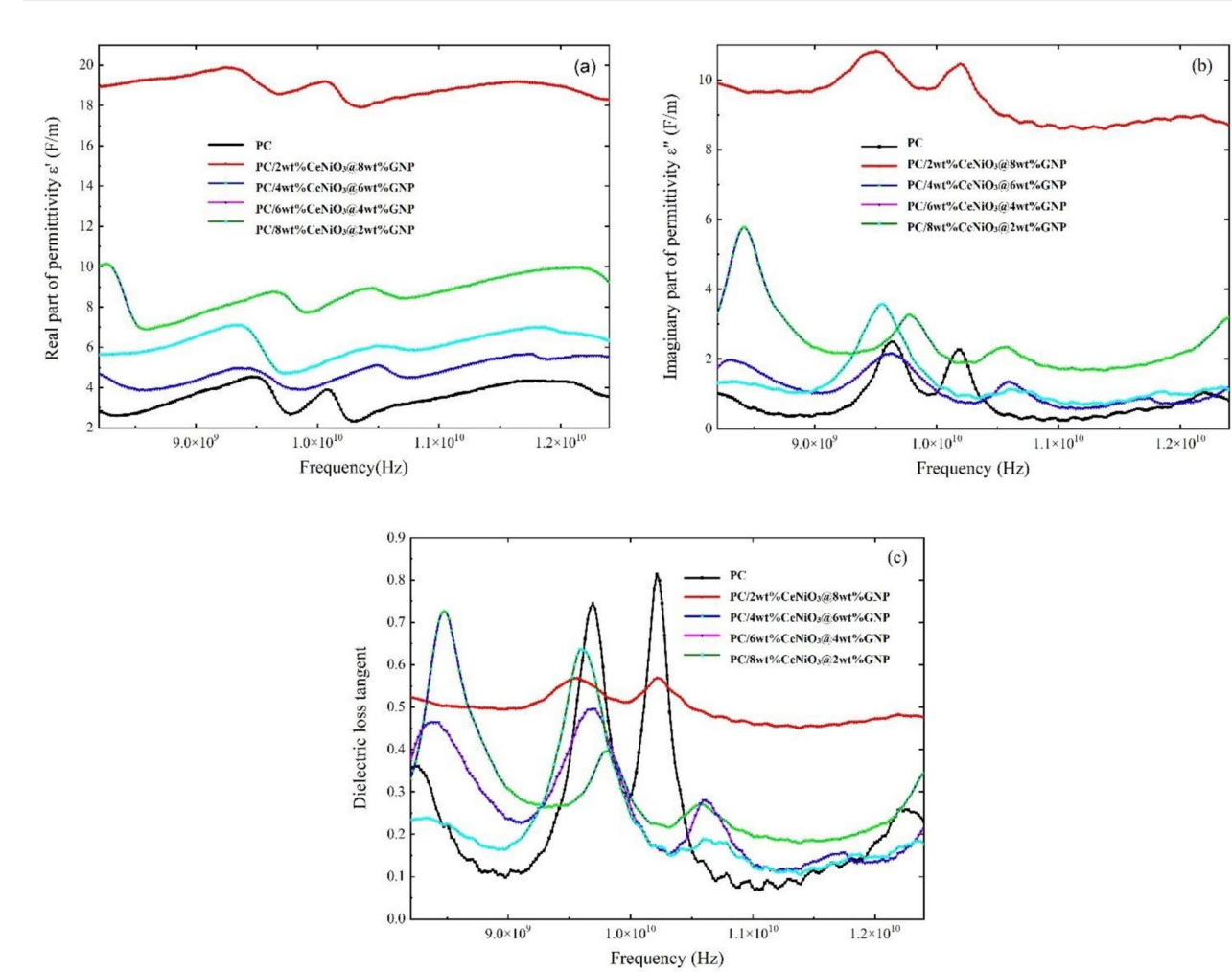


Fig. 9 a Real part of permittivity. b Imaginary part of permittivity. c Dielectric loss tangent of PC/CeNiO<sub>3</sub>@GNP

M. et al. J Mater. Sci: Mater Eng. (2025) 20:142 Page 11 of 13

## Magnetic loss tangent

The real part of permeability ( $\mu'$ ) represents the material's ability to store magnetic energy. The graph variations of permeability depending on the composition of CeNiO<sub>3</sub> and GNP are shown in. The pristine PC film exhibits moderate permeability, while composites with CeNiO<sub>3</sub> and GNP show increased or decreased  $\mu'$  at certain frequencies. The permeability peaks suggest resonance effects, indicating how the composite interacts with the electromagnetic waves.

The imaginary part of permeability  $(\mu'')$  represents magnetic energy dissipation. Figure 10b indicates the variation of  $\mu''$  versus frequency; higher  $\mu''$  means more energy is absorbed and converted into heat, which is beneficial for EMI shielding. The polymer nanocomposite

with 6 wt%, 4 wt% and 8 wt%, 2 wt% exhibits high initial  $\mu^{\prime\prime}$  values, suggesting strong energy dissipation at lower frequencies. Peaks around  $9\times10^9$  Hz and  $10^{10}$  Hz indicate resonance phenomena, like the real permeability trends. The presence of GNP influences loss behavior, as it enhances electrical conductivity and thus affects eddy current losses.

The magnetic loss tangent (tan  $\delta_M$ ) is directly related to the real ( $\mu'$ ) and imaginary ( $\mu''$ ) parts of permittivity through the equation:

$$tan \delta M = \frac{\mu''}{\mu'} \tag{7}$$

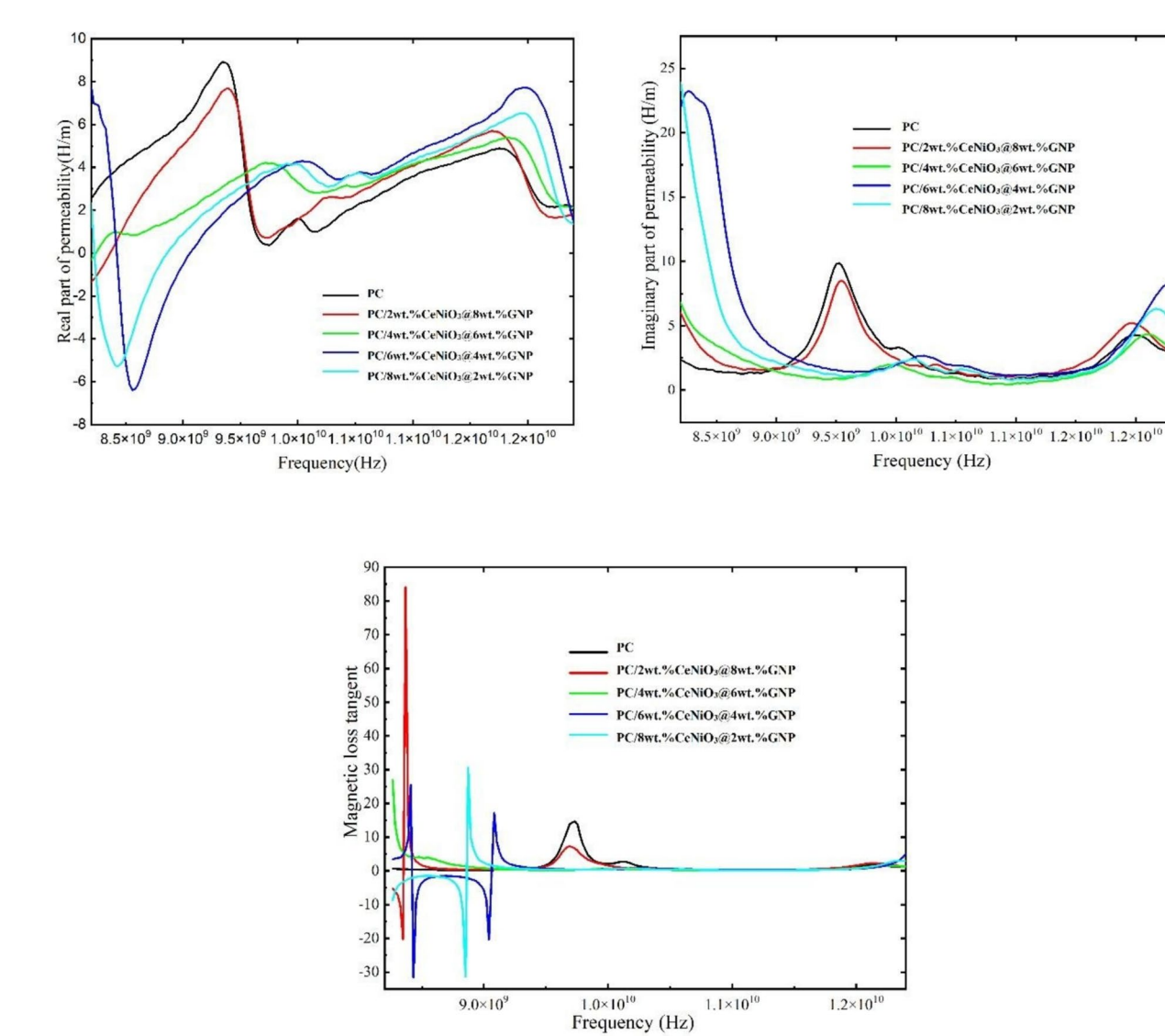


Fig. 10 a Real part of permeability. b Imaginary part of permeability. c Magnetic loss tangent of PC/CeNiO<sub>3</sub>@GNP

M. et al. J Mater. Sci: Mater Enq. (2025) 20:142 Page 12 of 13

Magnetic loss tangent quantifies the material's efficiency in absorbing electromagnetic energy. The higher values indicate better EMI shielding performance, as more energy is dissipated rather than reflected. Compositions with higher CeNiO $_3$  show increased fluctuations, indicating stronger magnetic interactions. The higher  $\mu^{'}$  and  $\mu^{''}$  together lead to good shielding effectiveness because the material can absorb and dissipate electromagnetic waves effectively. The loss tangent peaks indicate optimal frequency ranges where the composite materials provide the best EMI shielding.

## Conclusion

The study demonstrates that the incorporation of CeNiO<sub>3</sub> and GNP into the polycarbonate (PC) matrix significantly enhances the EMI shielding effectiveness of the nanocomposites. The polymer nanocomposites were fabricated using a solution casting method. Morphological studies via SEM and EDX confirmed uniform dispersion of nanofillers and their successful integration within the polymer matrix. The XRD analysis revealed the presence of both CeNiO<sub>3</sub> and GNP crystalline phases along with a reduction in the polymer's amorphous peak intensity, indicating filler-polymer interaction. The FTIR spectroscopy showed noticeable changes in characteristic absorption bands, further confirming the interaction between the polymer and nanofillers. The nanocomposites exhibited improved AC conductivity with increasing GNP content due to the formation of effective conductive pathways. The highest EMI shielding effectiveness (SE<sub>T</sub>~36 dB at 8.39 GHz) was observed for the sample containing 4 wt% CeNiO<sub>3</sub> and 6 wt% GNP, demonstrating an optimal balance between reflection (SE<sub>R</sub>) and absorption (SE<sub>A</sub>). Dielectric and magnetic loss tangent analyses confirmed that both interfacial polarization and magnetic resonance contribute to enhanced energy dissipation, especially in the 9-10 GHz range. Overall, the synergistic combination of CeNiO<sub>3</sub> for dielectric and magnetic losses and GNP for electrical conductivity and reflection offers a promising strategy for developing high-performance EMI shielding materials. The balanced formulation of 4 wt% CeNiO<sub>3</sub> and 6 wt% GNP in PC was identified as the most effective, making it suitable for broadband EMI shielding applications, particularly in the X-band frequency range. In future, we will explore the optimization of filler ratios, scalable processing, and extending frequency testing to achieve broadband EMI shielding. In addition, mechanistic studies and sustainable synthesis approaches will be pursued to broaden the applicability of PC/CeNiO<sub>3</sub>@GNP nanocomposites in advanced electronics, aerospace, and flexible wearable systems.

#### Authors' contributions

Supreetha M: conceptualization, methodology, software. Madhukar B S: conceptualization, methodology. Veena M.G: data curation, writing—original draft, supervision, software, validation. Pawandeep Kaur: writing—review and editing. Gnana Prakash A P: writing—review and editing, supervision.

### Funding

The authors did not receive any specific grant from any public and private funding agencies for this research work.

## Data availability

No datasets were generated or analyzed during the current study.

## **Declarations**

### **Competing interests**

The authors declare that they have no competing interests.

Received: 13 August 2025 Accepted: 13 October 2025 Published online: 14 November 2025

## References

Arjmand M, Mahmoodi M, Gelves GA, Park S, Sundararaj U (2011) Electrical and electromagnetic interference shielding properties of flow-induced oriented carbon nanotubes in polycarbonate. Carbon 49(11):3430–3440. https://doi.org/10.1016/j.carbon.2011.04.039

Bagotia N, Choudhary V, Sharma DK (2017) Studies on toughened polycarbonate/multiwalled carbon nanotubes nanocomposites. Compos Part B-Eng 124:101–110. https://doi.org/10.1016/j.compositesb.2017.05.037

- Bagotia N, Choudhary V, Sharma DK (2018) Superior electrical, mechanical and electromagnetic interference shielding properties of polycarbonate/ethylene- methyl acrylate-in situ reduced graphene oxide nanocomposites. J Mater Sci 53(23):16047–16061. https://doi.org/10.1007/s10853-018-2749-7
- Bagotia N, Choudhary V, Sharma DK (2019) Synergistic effect of graphene/ multiwalled carbon nanotube hybrid fillers on mechanical, electrical and EMI shielding properties of polycarbonate/ethylene methyl acrylate nanocomposites. Compos Part B 159:378–388. https://doi.org/10.1016/j. compositesb.2018.10.009
- Barad H-N, Keller DA, Rietwyk KJ, Ginsburg A, Tirosh S, Meir S, Anderson AY, Zaban A (2018) How transparent oxides gain some color: discovery of a CeNiO3 reduced bandgap phase as an absorber for photovoltaics. ACS Comb Sci 20(6):366–376. https://doi.org/10.1021/acscombsci.8b00031
- Bhaskaran K, Bheema RK, Etika KC (2020) The influence of Fe3O4@GNP hybrids on enhancing the EMI shielding effectiveness of epoxy composites in the X-band. Synth Met 265:116374. https://doi.org/10.1016/j.synthmet.2020. 116374
- Bheema RK, Ojha AK, Praveen Kumar AV, Etika KC (2022) Synergistic influence of barium hexaferrite nanoparticles for enhancing the EMI shielding performance of GNP/epoxy nanocomposites. J Mater Sci 57(19):8714–8726. https://doi.org/10.1007/s10853-022-07214-8
- Choudhary HK, Kumar R, Pawar SP, Bose S, Sahoo B (2020) Effect of microstructure and magnetic properties of Ba-Pb-hexaferrite particles on EMI shielding behavior of Ba-Pb-hexaferrite-polyaniline-wax nanocomposites. J Electron Mater 49(3):1618–1629. https://doi.org/10.1007/ s11664-019-07478-y
- Dehghani F, Ayatollahi S, Bahadorikhalili S et al (2020) Synthesis and characterization of mixed–metal oxide nanoparticles (CeNiO $_3$ , CeZrO $_4$ , CeCaO $_3$ ) and application in adsorption and catalytic oxidation–decomposition of asphaltenes with different chemical structures. Pet Chem 60:731–743. https://doi.org/10.1134/S0965544120070038
- Erdogan N, Erden F, Astarlioglu AT, Ozdemir M, Ozbay S, Aygun G, Ozyuzer L (2020) ITO/au/ITO multilayer thin films on transparent polycarbonate with enhanced EMI shielding properties. Curr Appl Phys 20(4):489–497. https://doi.org/10.1016/j.cap.2020.01.012
- Gedler G, Antunes M, Velasco JI, Ozisik R (2016) Enhanced electromagnetic interference shielding effectiveness of polycarbonate/graphene

M. et al. J Mater. Sci: Mater Enq. (2025) 20:142 Page 13 of 13

- nanocomposites foamed via 1-step supercritical carbon dioxide process. Mater des 90:906–914. https://doi.org/10.1016/j.matdes.2015.11.021
- Lee YS, Lee JH, Yoon KH (2021) EMI shielding and mechanical properties of polycarbonate nanocomposites containing CNT composite powder. Fibers Polym 22:1704–1710. https://doi.org/10.1007/s12221-021-0662-1
- Maiti S, Khatua BB (2016) Graphene nanoplate and multiwall carbon nanotube– embedded polycarbonate hybrid composites: high electromagnetic interference shielding with low percolation threshold. Polym Compos 37(7):2058–2069. https://doi.org/10.1002/pc.23384
- Maiti S, Suin S, Shrivastava NK, Khatua BB (2014) A strategy to achieve high electromagnetic interference shielding and ultra low percolation in multiwall carbon nanotube–polycarbonate composites through selective localization of carbon nanotubes. RSC Adv 4(16):7979–7990
- Pratik Nimbalkar, Amit Korde, R.K. Goyal, Electromagnetic interference shielding of polycarbonate/GNP nanocomposites in X-band, Materials Chemistry and Physics, Volume 206, 2018, Pages 251–258, ISSN 0254–0584, https://doi.org/10.1016/j.matchemphys.2017.12.027.
- Pande S, Chaudhary A, Patel D, Singh BP, Mathur RB (2014) Mechanical and electrical properties of multiwall carbon nanotube/polycarbonate composites for electrostatic discharge and electromagnetic interference shielding applications. RSC Adv 4(27):13839–13849. https://doi.org/10.1039/C3RA47387B
- Pasha A, Khasim S, Manjunatha SO (2023) Highly efficient EMI shielding applications of porous nickel–iron ferrite doped with yttrium nanocomposite thin films as a multifunctional material. J Mater Sci Mater Electron 34:409. https://doi.org/10.1007/s10854-023-09844-3
- Quy-Dat Nguyen, Choon-Gi Choi, Recent advances in multifunctional electromagnetic interference shielding materials, Heliyon, Volume 10, Issue 10,2024, e31118, ISSN 2405–8440, https://doi.org/10.1016/j.heliyon.2024.e31118.
- Rajesh Kumar B, Etika KC (2022) Facile one-pot hydrothermal synthesis of copper nanowires and their impact on the EMI shielding capability of epoxy composites. Chem Eng Technol 45(3):410–416. https://doi.org/10.1002/ceat
- Rajesh Kumar Bheema, Gopu J, Krithika Bhaskaran, Akshat Verma, Murthy Chavali, Krishna Chaitanya Etika, A review on recent progress in polymer composites for effective electromagnetic interference shielding properties structures, process, and sustainability approaches, Nanoscale Advances, Volume 6, Issue 23,2024,Pages 5773–5802,ISSN 2516–0230,https://doi.org/10.1039/d4na00572d.
- Ramakrishna BN, Pasha Ā, Khasim S (2024) Improved broadband electromagnetic interference shielding and strain sensing properties of multifunctional reduced graphene oxide/iron–cobalt ferrite composites. J Mater Sci Mater Electron 35:48. https://doi.org/10.1007/s10854-023-11781-0
- Rani P, Khadheer Pasha SK (2024) A study of EMI shielding efficiency, dielectric, and impedance properties of polymer nanocomposites reinforced with Graphene nanoplatelets, montmorillonite, and copper oxide nanoparticles. Polymer-Plastics Technology and Materials 63(16):2258–2275. https://doi.org/10.1080/25740881.2024.2369680
- Rashad M, Pan F, Tang A et al (2014) Development of magnesium-graphene nanoplatelets composite. J Compos Mater 49(3):285–293. https://doi.org/10.1177/0021998313518360
- Sankaran S, Deshmukh K, Ahamed MB, Khadheer Pasha SK (2018) Recent advances in electromagnetic interference shielding properties of metal and carbon filler reinforced flexible polymer composites: a review. Compos Part A Appl Sci Manuf 114:49–71. https://doi.org/10.1016/j.compo sitesa.2018.08.006
- Tong XC (2009) Advanced Materials and Design for Electromagnetic Interference Shielding (1st ed.). CRC Press. https://doi.org/10.1201/9781420073
- V. Uma Varun, B. Rajesh Kumar and K. C. Etika, Hybrid polymer nanocomposites as EMI shielding materials in the X-band, Mater. Today: Proc., 2019, 28, 796–798, https://doi.org/10.1016/j.matpr.2019.12.300.
- Vyas MK, Chandra A (2019) Synergistic effect of conducting and insulating fillers in polymer nanocomposite films for attenuation of X-band. J Mater Sci 54(2):1304–1325. https://doi.org/10.1007/s10853-018-2894-z
- Wang Tong, Hu Jiacong, Yang Haibo, Jin Li, Wei Xiaoyong, Li Chunchun, Yan Fei, Lin Ying (2017) Dielectric relaxation and Maxwell-Wagner interface polarization in  ${\rm Nb_2O_5}$  doped  $0.65{\rm BiFeO_3}$ – $0.35{\rm BaTiO_3}$  ceramics. J Appl Phys 121(8):084103. https://doi.org/10.1063/1.4977107

Yu W-C, Wang T, Liu Y-H, Wang Z-G, Xu L, Tang J-H, Dai K, Duan H-J, Xu J-Z, Li Z-M (2020) Superior and highly absorbed electromagnetic interference shielding performance achieved by designing the reflection-absorption-integrated shielding compartment with conductive wall and lossy core. Chem Eng J 393:124644. https://doi.org/10.1016/j.cej.2020.124644

Zhang B (2019) Double-shell PANS@PANI@Ag hollow microspheres and graphene dispersed in epoxy with enhanced microwave absorption.

J Mater Sci Mater Electron 30(10):9785–9797. https://doi.org/10.1007/s10854-019-01315-y

# **Publisher's Note**

Springer Nature remains neutral with regard to jurisdictional claims in published maps and institutional affiliations.